



Adsorption and Thermodynamics Behaviors of Ferroin [tris(1,10-phenanthroline Iron(II) Sulphate Complex] as Corrosion Inhibitor for Mild Steel in Acidic Medium

Shefali Dahiya¹ and Suman Lata^{1*}

¹Department of Chemistry, Deenbandhu Chhotu Ram University of Science and Technology, Murthal, Haryana, India.

Authors' contributions

This work was carried out in collaboration between both authors. Both authors read and approved the final manuscript.

Article Information

DOI: 10.9734/ACSJ/2016/21414

Editor(s):

- (1) Ling Bing Kong, School of Materials Science and Engineering, Nanyang Technological University, Singapore.
(2) Francisco Marquez-Linares, Full Professor of Chemistry, Nanomaterials Research Group, School of Science and Technology, University of Turabo, USA.

Reviewers:

- (1) Hao Wang, Northeastern University, P. R. China.
(2) Anonymous, Central University, New Delhi, India.

Complete Peer review History: <http://sciencedomain.org/review-history/11808>

Original Research Article

Received 16th August 2015
Accepted 23rd September 2015
Published 12th October 2015

ABSTRACT

The inhibition effect of Ferroin solution [tris(1,10-phenanthroline iron(II) sulphate complex] as a corrosion inhibitor was analysed against corrosion of mild steel (MS) in 0.5 M HCl solution, by using weight loss method, linear polarization, electrochemical impedance spectroscopy and scanning electron microscopic. The weight loss study of MS samples has proved that the reagent used was an efficient corrosion inhibitor with inhibition efficiency of >90%. The mixed mode of inhibition was confirmed by electrochemical polarizations. The results of electrochemical impedance spectroscopy have shown the changes in the impedance parameters, like R_{ct} and C_{dl} , which confirmed the adsorption phenomenon taking place on the MS surface. The inhibition action of the compound was assumed to occur through adsorption on the steel surface at the active centers present in the inhibitor.

Keywords: Ferroin solution; mild steel; linear polarization; EIS; SEM; corrosion.

*Corresponding author: E-mail: sumanjakhar.chem@dcrustm.org;

1. INTRODUCTION

Mild steel is widely applied in buildings, pipelines, bridges, vehicles, storage tanks for industrial water and wastewater systems and even in home appliances, due to its low cost and remarkably excellent mechanical properties. However, the major problem of its application is the dissolution of iron metal in acidic solutions, when using for acid pickling, industrial acid cleaning, acid descaling and oil well acidizing processes. Corrosion is the dissolution of metal, which is a slow and silent toxin for the industries using iron metal and alloys, hence, addressing this problem becomes a hot research topic. Recently, the inhibition of mild steel corrosion in acid solutions by using different types of organic inhibitors has been extensively studied [1-4], as the use of inhibitors is the most economical and practical method to reduce corrosive attack on metals [5-7]. The protection of metals from corrosion using safe corrosion inhibitors in the acidic medium is the basic aim of this research. The inhibitors are some chemical compounds which inhibit the metal against corrosion by interacting with the metallic surface or surrounding environment. Moreover, it has been a continuous struggle to discover those compounds with greater efficiency of inhibition in the acidic medium. The conventional inhibitors are organic compounds having heteroatoms (N, S, O, P) in their aromatic or long carbon chained structures. Such compounds are adsorbed on the metal surface, thereby blocking its active sites and thus resulting in reaction to inhibit the corrosion. The adsorption of corrosion inhibitors is mainly due to the physico-chemical characters of the inhibiting molecule, due to their functional groups, steric factors, aromaticity, p-orbital character of donating electrons, π -electron density at the donor atoms. They mainly have centers which contribute to the formation of a protective layer, through donation of their electron density towards the metal surface [8-10]. The present study aims to investigate inhibitive properties of a reagent Ferroin solution to prevent the corrosion of mild steel.

2. EXPERIMENTAL

2.1 Materials

The aggressive solution 0.5 M HCl was prepared by dilution of analytical grade HCl with double distilled water. All experiments were carried out in unstirred solutions. Before all measurements, mild steel specimens, having composition (wt%)

0.14 C, 0.03 Si, 0.032 Mn, 0.05 S, 0.20 P, 0.01 Ni, 0.01 Cu, 0.01 Cr and balanced Fe, were abraded successively with emery papers from 600 to 1200 grade. The specimen were then washed thoroughly with double distilled water, degreased with acetone and finally dried. After drying, the specimen were placed in desiccator and used for experiment. Rectangular specimens with dimension of 1.0× 1.0 × 0.5 cm were used in weight loss experiments and surface microscopy, while samples with size of 1.0 cm × 1.0 cm (exposed) were used for electrochemical measurements. The inhibitor used is a reagent, Ferroin [tris(1,10-phenanthroline iron (II) sulphate complex] red coloured compound in its reduced form with molecular formula $C_{36}H_{24}FeN_6O_4S$.

2.2 Gravimetric Analysis

For weight loss experiments, the polished and dried specimens were weighed before and after immersion in 0.5 M HCl for 4 h in the absence and presence of the inhibitor at different temperatures (303 K, 313 K, 323 K and 333 K), in inhibitor solutions with different concentrations (200 ppm, 400 ppm, 800 ppm and 1000 ppm). Each experiment was conducted for two times to calculate the inhibition efficiency.

2.3 Polarisation Measurements

Polarization measurements were performed at the temperatures similarly to those of the weight loss experiments. For polarization measurements, a conventional three electrode Pyrex glass cell, consisting of a saturated calomel electrode (SCE) as reference electrode, the mild steel specimen as working electrode and a platinum foil as counter electrode, was used. All electrodes were dipped in the same test solutions with a Luggin capillary bridge arrangement to minimize resistance polarization. The experiment was carried out using the CHI760C electrochemical analyser and in thermostatic controlled water baths at constant temperature (± 0.5 K). The anodic and cathodic polarization values were measured under galvanostatic conditions and the corresponding Tafel lines were constructed that provided the data for calculating the corrosion rates and efficiencies of the inhibitors.

2.4 Electrochemical Impedence Spectroscopy

EIS is a special and reliable laboratory technique, with the applicable software to

determine significant parameters like the charge transfer resistance (R_{ct}) rate and double-layer capacitance (C_{dl}) [11]. The AC impedance measurements were carried out in the range of 1.0×10^5 -1.0 Hz with the AC signal 5 mV peak-to-peak. The same cell and system as in the polarization method were used. The double-layer capacitance (C_{dl}) and the charge transfer resistance (R_{ct}) were calculated from Nyquist plots.

2.5 SEM Studies

SEM studies were performed on the coupons immersed in the acidic medium both in the absence and presence of Feroin at a concentration of 1000 ppm. The coupons were immersed for 4hr duration at 303 K. The coupons were thoroughly polished using range of emery papers, washed and dried in acetone, similar to weight loss experiment. After the time duration coupons were rubbed to scale off the corroded layer and then, again washed and dried. SEM studies were performed by using Model Zeiss Ultra 55 microscopy.

3. RESULTS AND DISCUSSION

3.1 Gravimetric Analysis

The inhibition efficiency of the inhibitor (Table.1), calculated by using the following equation, increases with increasing concentration in the acidic medium and a decrease in efficiency is observed with the increasing range of temperature.

$$\eta\% = \frac{W - W_{inh}}{W} \times 100, \quad (1)$$

$$CR(mmpy) = \frac{W - W_{inh}}{DAT} \times 87.6, \quad (2)$$

where, W is the weight loss in blank solution i.e. in absence of inhibitor (g), W_{inh} is the weight loss in presence of the inhibitor (g), D is the density of metal ($g \cdot cm^{-3}$), A is the exposed area of the metal (cm^2) and T is the exposure time in (h) [12]. Fig. 1 shows the plot of corrosion rate (mmpy) against inhibitor concentration (ppm) for the corrosion of mild steel in 0.5 M HCl in the range of increasing temperatures from 303 K to 333 K. The figure showed that the corrosion rate, calculated from Eq. (2), decreases as the concentration of the inhibitor increases in addition to the increasing trend of corrosion rate with increasing temperature.

3.2 Polarisation Measurements

To study the effect of Feroin solution on the polarization behavior of MS and to analyze the inhibition action of reagent on steel corrosion in 0.5 M HCl, polarization curves for different concentrations of inhibitor were plotted. Figs. 2 and 3 presents polarization curves for mild-steel electrode in 0.5 M HCl, in the absence and presence of inhibitor at different concentrations. The electrochemical parameters obtained from polarization measurements are listed in Table 2. From the plot and the table, it is clear that both cathodic and anodic reactions on mild-steel electrode have been inhibited in the presence of the studied compound. Electrochemical corrosion parameters including corrosion potential (E_{corr}), cathodic and anodic Tafel slopes (β_c , β_a), and corrosion current density (I_{corr}), obtained by extrapolation of Tafel lines, are given in Table 2. The inhibition efficiency ($\% \eta$), was calculated from the following equation [13]:

$$\% \eta = \frac{I_{corr} - I_{corr}^0}{I_{corr}} \times 100, \quad (3)$$

where, I_{corr} and I_{corr}^0 are the values of corrosion current densities without and with the inhibitor, respectively, which were determined by extrapolation of the cathodic and anodic Tafel curve [14]. The E_{corr} values from the polarization diagrams show that the inhibitor behaves as a mixed type, with small variations in the E_{corr} values of the blank specimens.

3.3 Electrochemical Impedance Spectroscopy

The corrosion behavior of MS in 0.5 M HCl solution in the absence and presence of the reagent was investigated using electrochemical impedance spectroscopy (EIS). Nyquist plots of MS in absence and presence of inhibitor solutions in various concentrations of inhibitor are given in Fig. 4(a) along with equivalent circuit diagram in Fig. 4(b). It is observed, the impedance response of MS in blank solution significantly changed after addition of inhibitor. The values of inhibition efficiency ($\% \eta$) were calculated by following the equation [15]:

$$\% \eta = \frac{R_{ct}^0 - R_{ct}}{R_{ct}^0} \times 100 \quad (4)$$

Where, R_{ct} and R_{ct}^0 are the charge transfer resistances ($ohm \cdot cm^2$) values in the absence and presence of the inhibitors, respectively. To obtain

the values of double-layer capacitance (C_{dl}), the values of frequency at which the maximum imaginary component of the impedance f_{max} were found and were used in the following equation with corresponding R_{ct} values [15]:

$$C_{dl} = \frac{1}{2\pi f_{max} R_{ct}} \quad (5)$$

Nyquist plots shows depressed semi-circles with the center under the real axis, whose size increased with the increase in concentration of the inhibitor, confirming that the charge transfer processes were mainly controlling the corrosion of MS. Table 3 reveals that the value of R_{ct}

increases prominently with the increase in the inhibitor concentration, while the value of C_{dl} is decreased. This indicates an increase in the surface coverage by adsorption of the inhibitor on the MS, which results in the increase in inhibitor efficiency and the maximum reaches up to 90%. The decrease in the C_{dl} related to the decrease in local dielectric constant or an increase in the thickness of the electrical double layer, suggests that inhibitor molecules function by adsorption at the interface of metal/solution [16]. Hence, the molecules replace the water molecules gradually by adsorbing at metal / solution interface, leading to the decrease in the extent of dissolution reaction.

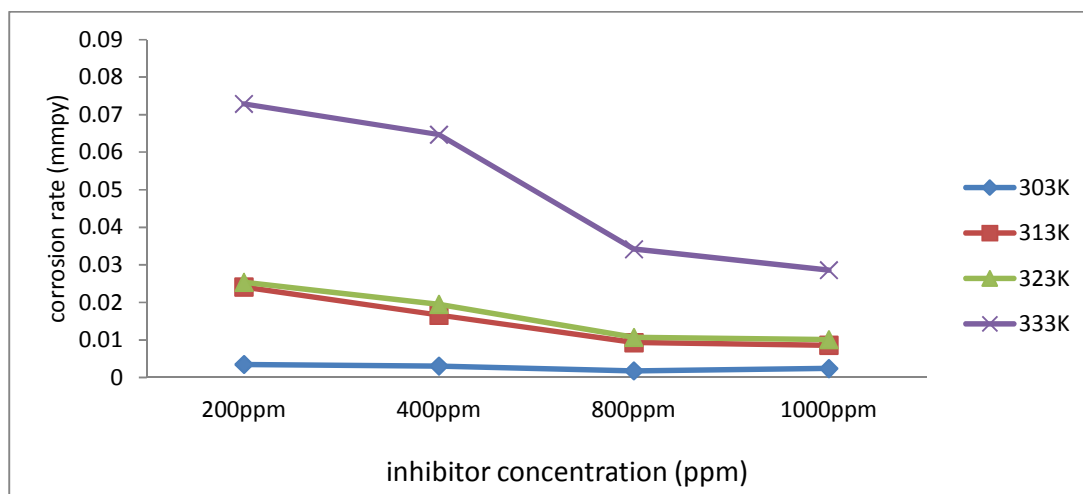


Fig. 1. Plot between corrosion rate and inhibitor concentrations (200 ppm, 400 ppm, 800 ppm and 1000 ppm) at varying temperatures

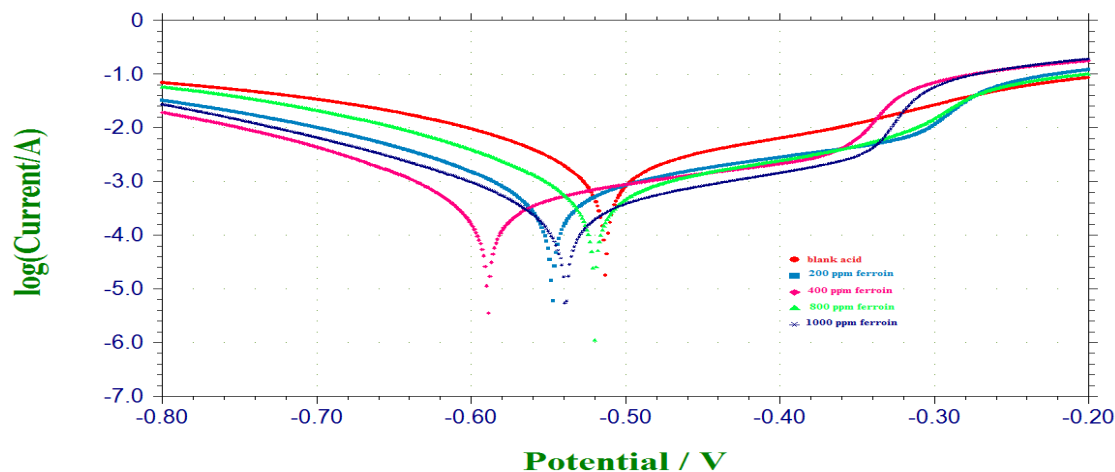


Fig. 2. Tafel curve at 303 K in absence and presence of Ferrioin at 200 ppm, 400 ppm, 800 ppm and 1000 ppm concentrations

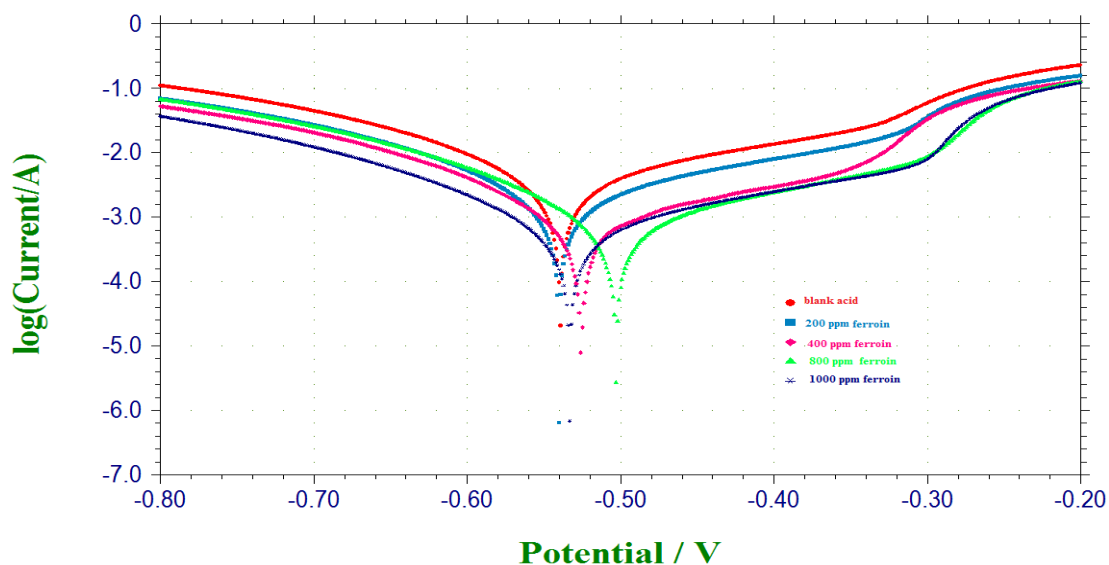


Fig. 3. Tafel curve at 313K in absence and presence of ferriin at 200 ppm, 400 ppm, 800 ppm and 1000 ppm concentrations

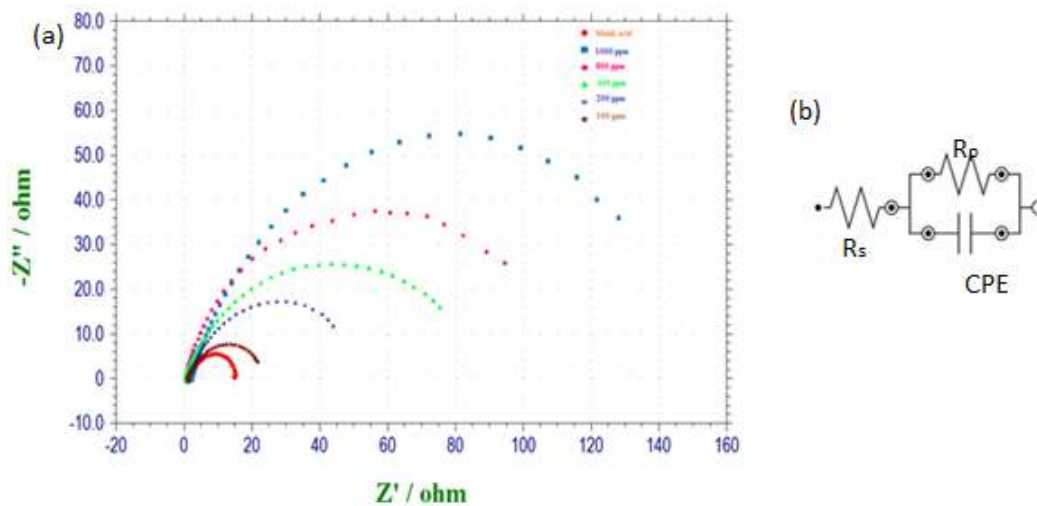


Fig. 4(a). Nyquist plots in absence and presence of ferriin in acidic medium at varying concentration and (b) Equivalent circuit diagram of EIS study

Table 1. Inhibition efficiency of ferriin at MS surface at 303K, 313K, 323K and 333K

Temperature (K)	Inhibition efficiency of ferriin solution (%)			
	200 ppm	400 ppm	800 ppm	1000 ppm
303	90.33	90.7	92.03	92.56
313	81.9	82.36	83.75	83.74
323	47.51	78.41	78.8	81.23
333	39.9	46.74	74.84	76.42

Table 2. Polarisation data at varying concentrations (200 ppm, 400 ppm, 800 ppm and 1000 ppm) and at 303K, 313K, 323K and 333K) temperatures from Tafel plots showing anodic and cathodic slopes, E_{corr} and I_{corr} values

Temperature (K)	Conc. of inhibitor (ppm)	$E_{corr} \times 1000$ (-mV)	β_a (mV/dec)	β_b (mV/dec)	I_{corr} (mA cm^{-2})	% η
303	0	513	192.23	131.87	2.218	-
	200	520	198.8	109.22	0.618	72.14
	400	589	220.75	107.61	0.4405	80.14
	800	540	183.18	103.8	0.3928	82.3
	1000	539	189.75	112.84	0.3127	85.9
313	0	539	205.67	131.98	3.95	-
	200	533	220.26	117.75	1.118	71.69
	400	526	206.01	117.72	1.004	74.58
	800	503	195.16	114.71	0.859	78.25
	1000	533	198.02	117.61	0.682	82.73
323	0	543	196.15	205.97	17.41	-
	200	532	178.25	215.36	5.623	69.02
	400	523	142.67	226.44	4.795	72.46
	800	546	141.96	207.25	3.837	77.96
	1000	528	139.87	216.87	3.566	79.52
333	0	517	213.72	170.12	19.08	-
	200	546	208.94	161.1	6.031	68.39
	400	508	213.72	164.09	7.82	73.29
	800	524	231.69	136.27	4.705	75.34
	1000	558	208.24	143.49	3.559	81.34

Table 3. EIS data showing increase in inhibition efficiency (% η) with variation in charge transfer resistance (R_{ct}) and double-layer capacitance (C_{dl})

Concentration of inhibitor	R_{ct} / Ohm cm^2	C_{dl} / μF cm^{-2}	I. E (%)
Blank	14.325	435.92	-
100 ppm	25.011	95.84	42.72
200 ppm	56.339	75.53	74.57
400 ppm	103.870	49.92	86.21
800 ppm	114.414	20.95	87.47
1000 ppm	154.610	11.78	90.73

It is also significant that the inhibition efficiencies obtained from weight loss measurements are different from electrochemical experiments. This phenomenon attributed to the suggestion that weight loss experiments give average corrosion rates, whereas the electrochemical experiments give instantaneous corrosion rates [15]. This is why all the data (Tables 1, 2 and 3) have a similar trend in the inhibition efficiencies. However, the inhibition efficiencies calculated from EIS measurements, potentiodynamic polarization measurements and weight loss measurements are different. In the presence of Ferrioin reagent, it increases with increasing concentration and decreases with increasing temperature. The electrochemical data are instantaneous and considered as the bases of adsorption calculations.

3.4 Scanning Electron Microscopy

The surface morphology of the MS specimens immersed in 0.5 M HCl in the presence and absence of the Ferrioin solution at 1000 ppm concentration were studied by using scanning electron microscopy (SEM). The immersion time of the electrodes for the SEM analysis was 4 h at 303 K temperature. SEM images of the uninhibited sample and the inhibited sample are shown in Figs. 5(a) and 5(b), respectively.

3.5 Adsorption Isotherms

The results show that, the weight loss decreases with the increasing inhibitor concentration and therefore, the inhibition efficiency increases. It can be concluded that this inhibitor acts through

adsorption on metal surface and formation of a barrier layer between metal and corrosive media. The adsorption isotherms can provide basic information on the interaction of inhibitor and metal surface. In order to obtain adsorption isotherm, the surface coverage values (θ), for different concentrations (C) of the inhibitor in 0.5 M HCl solution have been obtained from electrochemical measurements and tested graphically for fitting of a suitable adsorption isotherm. To confirm the adsorption of inhibitor on metal surface, different adsorption isotherms were studied like Langmuir, Tempkin and Freundlich.

The plots of C/θ versus C (Fig. 6) [17] yields a straight line with correlation coefficient (R^2) >0.99, yielding that the adsorption of the reagent obeys the Langmuir adsorption isotherm:

$$\frac{C}{\theta} = \frac{1}{K_{ads}} + C, \quad (6)$$

where C is inhibitor concentration, θ is the degree of surface coverage, and K_{ads} is the equilibrium constant for adsorption-desorption process. The value of the equilibrium constant, K_{ads} , was calculated from the reciprocal of the intercept of the isotherm line.

K_{ads} values can be calculated from the intercepts of the straight lines, is related to the standard free energy of adsorption, ΔG_{ads}^0 with following equations [18]:

$$\Delta G_{ads}^0 = -RT \ln 55.5 K_{ads}, \quad (7)$$

$$\Delta G_{ads}^0 = -2.303RT(\log 55.5 K_{ads}). \quad (8)$$

ΔG_{ads}^0 was calculated and found $-17.46 \text{ kJmol}^{-1}$. The negative value of ΔG_{ads}^0 indicates spontaneous adsorption of the inhibitor molecules on the MS surface which shows interaction between inhibitor molecules and metal surface. The value of ΔG_{ads}^0 is less than -40 kJmol^{-1} , indicating electrostatic interaction between the charged inhibitor molecules and the charged metal surface, i.e., physical adsorption [19,20]. The negative values indicate the spontaneity of the adsorption process and stability of the adsorbed layer on MS surface.

3.6 Effect of Temperature

To calculate the activation parameters of the corrosion process and to study the inhibition mechanism due to the temperature, polarization

measurements were performed at 303 K, 313 K, 323 K, 333 K range of temperatures, in the absence and presence of the inhibitor concentrations the Arrhenius plots were analysed.

The activation energy of the corrosion process could be determined using the Arrhenius equation [21]:

$$I_{corr} = k \exp\left(-\frac{E_a}{RT}\right), \quad (9)$$

where, I_{corr} is corrosion current density, obtained by extrapolation of the Tafel lines of experiments carried out at 303K, 313K, 323K, 333K temperatures. E_a is the activation energy, R is the gas constant, T is the absolute temperature and k is the pre-exponential factor. The values of E_a can be calculated from the slopes of the straight lines in Fig. 7(a), these values show an increase in the activation energies of the various mediums studied. The E_a value for acidic medium in absence of inhibitor changes from 66.80 kJ/mol to 77.27 kJ/mol with inhibitor, showing increase in the threshold energy in presence of Feroin in the acidic medium. The apparent activation energy (E_a) in the acid solution was found to increase and the extent of the increase is proportional to the temperature increase, indicating that the energy barrier for the corrosion reaction increases with the temperature. This increase shows the retardation of the corrosion process by adsorption of inhibitor over the surface, that is actually protected by Feroin and hence, the formation of activated complex is retarded. Since the barrier to cross is much higher the activated complex formation would be less, or say, needs greater energy to transform into the corrosion product, and hence shows inhibition.

Activation parameters like enthalpy (ΔH^\ddagger) and entropy (ΔS^\ddagger) for the dissolution of MS in the acid medium in the absence and presence of various concentrations of Feroin solution was calculated from the following equations [22]:

$$\log K = \frac{-\Delta H^\ddagger}{2.303RT} + \frac{\Delta S^\ddagger}{2.303R}, \quad (10)$$

$$\Delta G_{ads}^0 = \Delta H_{ads}^0 - T\Delta S^0, \quad (11)$$

where K represents slope from the langmuir isotherm, R is the universal gas constant, ΔH^\ddagger is the enthalpy of activation and ΔS^\ddagger is the entropy of activation. The plot of $\log k$ against $1/T$ Fig. 7(b), gave straight line with slope $-\Delta H^\ddagger$

$/2.303 R$ and intercept $\Delta S^{\ddagger}/2.303 R$ from which ΔH^{\ddagger} and ΔS^{\ddagger} values were calculated as 10.32 kJ/mol and -9.41 J/mol·K, respectively. Generally, an exothermic process signifies either physisorption or chemisorption or a combination of both. Typically, the enthalpy of physisorption process is lower than that of 40.00 kJ/mol while the enthalpy of chemisorptions process approaches 100 kJ/mol [23]. The entropy of activation (ΔS^{\ddagger}) for the inhibition process is negative, indicates that there is a decrease in randomness from reactants to the formation of activated complex [24].

3.7 Mechanism of Inhibition

The above observations and analysis show that the inhibitor is adsorbed on mild steel. Four mechanisms have been suggested for the adsorption of inhibitor at the metal–solution interface [25]. These are: (i) electrostatic attraction between charged molecules and charged metal, (ii) interaction of unshared electron pairs in the molecule with the metal, (iii) interaction of π -electrons with the metal and, and (iv) a combination of all of the above.

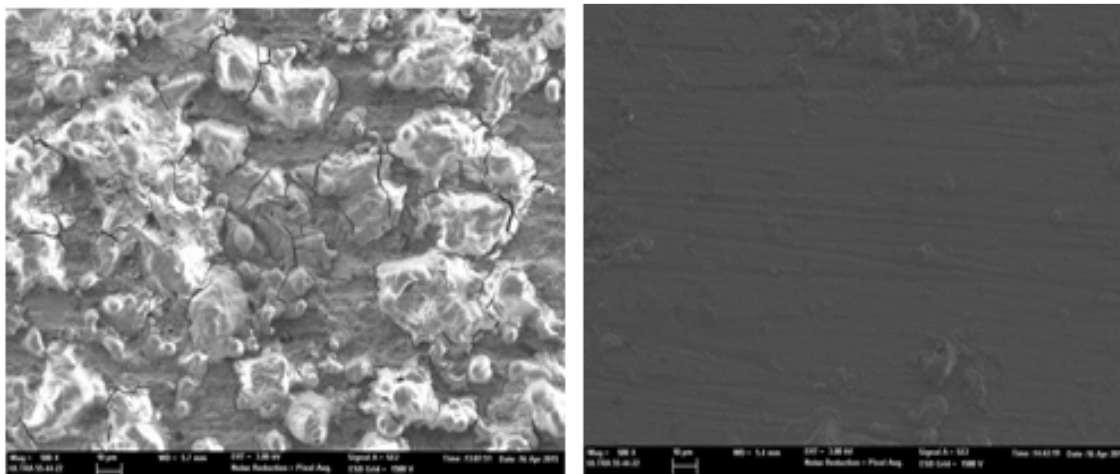


Fig. 5(a). SEM images of MS surface in acidic medium in the absence of ferrioin at 303K and 5(b). SEM images of MS surface in acidic medium in the presence of ferrioin (1000 ppm) at 303K

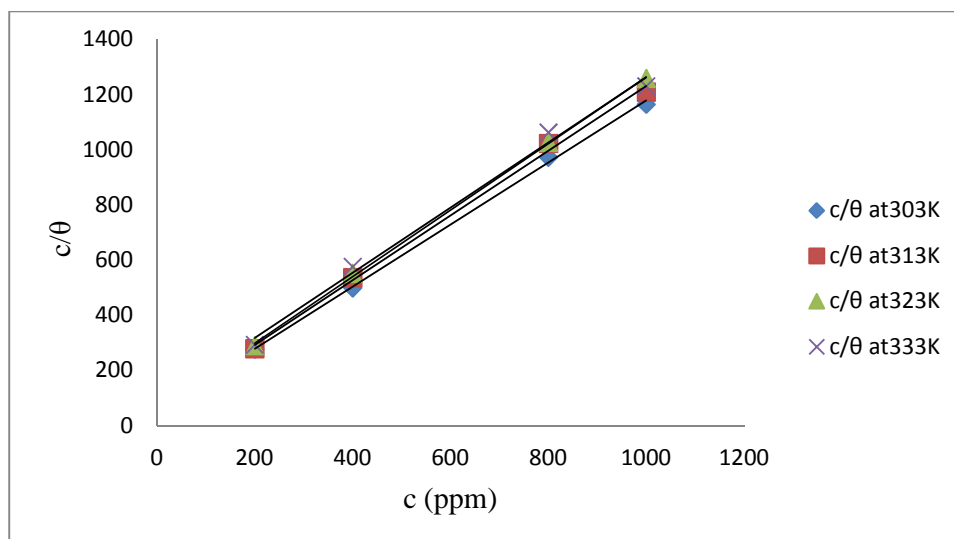


Fig. 6. Langmuir isotherm for ferrioin solution at range of temperatures (303K, 313K, 323K, 333K)

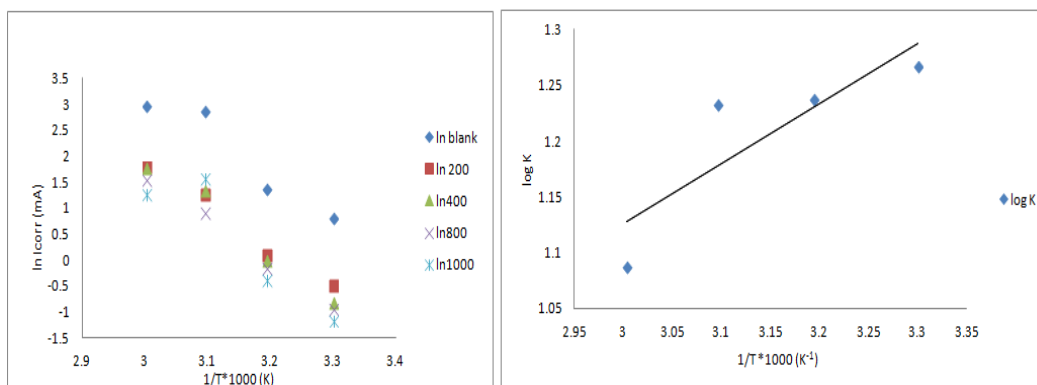


Fig. 7(a). Arrhenius plot of ferriion solution at varying concentrations of inhibitor (200 ppm, 400 ppm, 800 ppm, 1000 ppm) and 7(b). Plot between log K and 1/T for slope (ΔH°) and intercept (ΔS°)

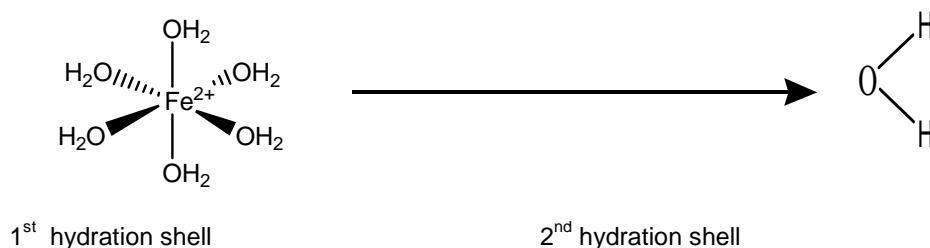
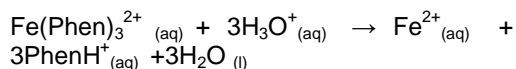


Fig. 8. Hydration sheath of Fe ion replaced by the inhibitor during adsorption process

Ferriion, a red coloured compound in its reduced form decolourizes in the acidic medium during the static experimental conditions. To explain this observation, it is expected that the Ferriion molecule undergoes dissociation in the acidic solution to give three protonated 1,10-Phenanthroline (Phen) moieties [26] as given in the reaction below:



Moreover, the hydration energy of Fe^{2+} ions [27] present in outer Helmholtz plane (OHP) [25] as well as in bulk and binding energy for Fe^{2+} ions and O^{2-} are comparable [28], as the former ions are bound to water molecules through oxygen in the hydration shell (Fig. 8) [29]. So, it may be expected that the cleavage of the primary hydration sheath in outer OHP as well as in bulk may take place because the number of water molecules in the first hydration sheath at the transition state is less than in the ground state, suggesting the dissociative mode of the activation state [30].

Simultaneously, the dissociation of Ferriion also takes place freeing Fe^{2+} ions. So, the possibility

to exchange of freed Fe^{2+} ions from their dismantled hydrated sheath with the similar ions coming from the dissociation of Ferriion arises in the acidic solution. The Phen moiety, in turn, bears electron rich sites and a planar geometry. This protonated Phen, Fe^{2+} from MS surface and Cl^- ions from HCl may bind together to form [Fe-Cl-protonated Phen]. These species may get adsorbed on the MS surface and hence hinder the corrosion reaction. Towards higher concentrations, Ferriion gives increased inhibition efficiency, shown in Table 1, may be attributed to the fact that on shifting from 200 ppm to 1000 ppm at intervals of 200 ppm of the inhibitor, there occurs a gradual enhancement in long range intermolecular interactions of attractive nature [31] and hence improves the extent of adsorption. The higher values of R_{ct} obtained at high concentrations also justify this concept. This phenomenon is more noticeable at lower temperatures.

At higher temperatures, the gradual decrease in efficiency in Table 2, can be explained on the basis of eliminating orientational forces of the inhibitor molecules at elevated temperatures. The inhibitor with electron rich centers, is expected to behave as a polar molecule as well

as MS interface containing Fe^{2+} ions, water dipoles, so long range dipole-dipole interaction may occur. Based upon the statistical calculations of dipole-dipole (dd) interactions by Reinganum [32] who proposed that on averaging all the orientations of dipole molecules (for example, inhibiting molecules and free Fe^{2+}) the orientational interaction energy becomes zero, i.e., $\langle E_{dd} \rangle = 0$, where bracket notation denotes an average over orientations and E is the energy corresponding to the probability of the dipole orientation obtained from Boltzmann factor $\exp(-E/RT)$. Also, without averaging, these orientational forces approach zero at higher temperatures, implies that with increasing temperatures, orientational forces become negligible, leaving behind the only van der Waals forces. These van der Waals forces at elevated temperatures [32] contributed the adsorption, but to a lesser extent. Hence, low efficiency is observed at higher temperatures.

4. CONCLUSIONS

Ferroun solution [tris(1,10-phenanthroline iron(II) sulphate complex] can be used as a corrosion inhibitor to prevent the corrosion of mild steel (MS). The studies were conducted with 0.5 M HCl solution by using weight loss method, linear polarization, electrochemical impedance spectroscopy and scanning electron microscopic studies. The inhibition efficiency of the inhibitor increased with increasing concentration and decreased with increasing temperature. Adsorption study showed that the inhibition mechanism obeyed Langmuir adsorption isotherm. The Tafel plots of polarization have shown that the Ferroun solution acted as a mixed type inhibitor. The results of the gravimetric analysis, electrochemical polarizations, and EIS were in very good agreement one another. SEM results clearly showed the formation of a protective film on the surface of mild steel.

ACKNOWLEDGEMENT

The authors are grateful to Professor Gurmeet Singh, University of Delhi, Delhi, India for providing the CHI760C electrochemical analyser.

COMPETING INTERESTS

Authors have declared that no competing interests exist.

REFERENCES

- Maksoud S, Abd El. The Effect of organic compounds on the electrochemical behaviour of steel in acidic media. Int J Electrochem Sci. 2008;3:528–55.
- Nasser JA, Sathiq MA. Adsorption and corrosion inhibition of mild steel in hydrochloric acid medium by N-[morpholin-4-yl(phenyl)methyl]benzamide. Int J Engg Sci & Tech. 2010;2(11):6417-26.
- Singh P, Bhrara K, Singh G. Adsorption and kinetic studies of L-leucine as an inhibitor on mild steel in acidic media. Appl Surf Sci. 2008;254:5927–35.
- Nor Zakiah Nor Hashim Karimah Kassim, Yusairie Mohd. (E)-N1-(4-Chlorobenzylidene)-N4-Phenylbenzene-1, 4-Diamine as Mild Steel Corrosion Inhibitor in 1M HCl. APCBEE Procedia. 2012;3: 239–44.
- Hari Kumar S, Karthikeyan S. Inhibition of mild steel corrosion in hydrochloric acid solution by cloxacillin drug. J Environ Sci. 2012;3(5):925–34.
- Olasehinde EF, Olusegun SJ, Adesina AS, Omogbehin SA, Momoh-Yahayah. Inhibitory action of *Nicotiana tabacum* extracts on the corrosion of mild steel in HCl: Adsorption and thermodynamics study. Nat Sci. 2013;11(1):83-90.
- Taleb H Ibrahim, Mohamed Abou Zour. Corrosion inhibition of mild steel using fig leaves extract in hydrochloric acid solution. Int J Electrochem Sci. 2011;6:6442-6455.
- Ade SB, Shithole NV, Lonkar SM. Antifungal drug's used as metal corrosion inhibitor in various acid medium. IJCRGG. 2014;6:3642-3650.
- Wanga X, Yang H, Wang F. Inhibition performance of a gemini surfactant and its co-adsorption effect with halides on mild steel in 0.25 M H_2SO_4 solution. Corros Sci. 2012;55:145-52.
- Gopi D, Govindaraju KM, Kavitha L. Investigation of triazole derived Schiff bases as corrosion inhibitors for mild steel in hydrochloric acid medium. J of Appl Electrochem. 2010;40:1349-56.
- Raja B, Sethuraman MG. Studies on the Inhibition of Mild Steel Corrosion by *Rauvolfia serpentina* in Acid Media. JMEPEG. 2009;19:761-6.
- Ilayaraja LG, Sasieekhumar AR, Dhanakodi P. Inhibition of mild steel corrosion in acidic medium by aqueous extract of *Tridax procumbens*. E-Journal of Chemistry. 2011;8:685-8.
- Soltani N, Behpour M, Ghoreishi SM, Naeimi H. Corrosion inhibition of mild steel in hydrochloric acid solution by some

- double Schiff bases. *Corros Sci.* 2010;51: 1351-61.
14. Ali Döner, Kardas G. N-aminorhodanine as an effective corrosion inhibitor for mild steel in 0.5 M H₂SO₄. *Corros Sci.* 2011;53: 4223-32.
 15. Singh A, Ebenso EE, Quraishi MA. Theoretical and electrochemical studies of metformin as corrosion inhibitor for mild steel in hydrochloric acid solution. *Int J Electrochem Sci.* 2012;7:4766-79.
 16. Al-Turkustania AM, Al-Sawata RM, Al-Hassania RM, Al-Ghamdia NS, Al-Harbia EM, Al-Gamdia MA, Al-Solmia SA. Corrosion behaviour of mild steel in acidic solution using the aqueous seed extract of *Phoenix dactylifera* L. (Date seeds). *J Chemica Acta.* 2013;2:53-61.
 17. Lata S, Chaudhary RS. Some triphosphates as corrosion inhibitor for mild steel in 3% NaCl solution. *Ind J Chem Tech.* 2008;15:364-74.
 18. Shukla SK, Ebenso EE. Corrosion inhibition, adsorption behavior and thermodynamic properties of streptomycin on mild steel in hydrochloric acid medium. *Int J Electrochem Sci.* 2011;6:3277-91.
 19. Tao ZZ, Shengtao Li W, Hou B. Corrosion inhibition of mild steel in acidic solution by some oxotriazole derivatives. *Corros Sci.* 2009;52:2588-99.
 20. Mistry BM, Patel NS, Patel MJ, Jauhari S. Corrosion inhibition performance of 1,3,5-triazinyl urea derivatives as a corrosion inhibitor for mild steel in 1 N HCl. *Res Chem Intermed.* 2011;37:659-671.
 21. Musa AY, Kadhum AAH, Mohamad AB, Rahoma AAB, Mesmari H. Electrochemical Study on Newly Synthesized Chloro-curcumin as an Inhibitor for Mild Steel Corrosion in Hydrochloric Acid. *J Mol Str.* 2013;6:5466-77.
 22. Garai S, Garai S, Jaisankar P, Singh J K, Elango A. A comprehensive study on crude methanolic extract of *Artemisia pallens* (Asteraceae) and its active component as effective corrosion inhibitors of mild steel in acid solution. *Corros Sci.* 2012;60:193-204.
 23. Kosari A, Momeni M, Parvizi R, Zakeri M, Moayed MH, Davoodi, Eshghi H. Theoretical and electrochemical assessment of inhibitive behavior of some thiophenol derivatives on mild steel in HCl. *Corros Sci.* 2011;53:3058-67.
 24. Ramesh SV, Adhikari AV. Inhibition of corrosion of mild steel in acid media by N0-benzylidene-3-(quinolin-4-ylthio) propane-hydrazide. *Iran J Chem Chem Eng.* 2009;31:699-711.
 25. John O'M Bockris, Amulya K. N. Reddy, Maria Gamboa-Aldeco. *Modern Electrochemistry 2A, Fundamentals of Electrodeics*, 2nd edn. Kluwer Academic: New York; 2000.
 26. Pandian, Raja B, Sethuraman MG. *Solanum tuberosum* as an inhibitor of mild steel corrosion in acid media. *Iran J Chem Chem Eng.* 2009;28:77-84.
 27. Leussing DL. Reaction of Ferrous and Ferric Iron with 1,10-Phenanthroline. I. dissociation constants of ferrous and ferric phenanthroline. *Jacs.* 1948;70:2348.
 28. Sattar SJ. A unified kinetics and equilibrium experiment: Rate law, activation energy, and equilibrium, Constant for the dissociation of ferroin. *Chem Educ.* 2011;88:457.
 29. Obi-Egbedi NO, Obot IB, El-Khaiary MI, Umoren SA, Ebenso EE. Computational simulation and statistical analysis on the relationship between corrosion inhibition efficiency and molecular structure of some phenanthroline derivatives on mild steel surface. *Int J Electrochem Sci.* 2011;6: 5649-5675.
 30. Mohammed AM. Hydration structure and water exchange dynamics of Fe(II) ion in aqueous solution. *Bull Chem Soc Etho.* 2010;24:239-250.
 31. Buckingham AD, Utting BD. *Annu Rev Phys Chem.* England: Univ. of Cambridge; 1970;21.
 32. Kaplan GL. *Intermolecular interactions: Physical picture, computational methods and model potentials.* New Jersey: Wiley; 2006.

© 2016 Dahiya and Lata; This is an Open Access article distributed under the terms of the Creative Commons Attribution License (<http://creativecommons.org/licenses/by/4.0>), which permits unrestricted use, distribution, and reproduction in any medium, provided the original work is properly cited.

Peer-review history:
 The peer review history for this paper can be accessed here:
<http://sciencedomain.org/review-history/11808>